Mansoura University
Faculty of Engineering
Mansoura Engineering Journal

Semi-Analytic modeling of laminar forced convection in a rectangular duct for arbitrary boundary conditions and inlet temperature profile

(نمذجة شبه تحليلية للحمل القسري الرقائقي في أنابيب ذات مقطع مستطيل تحت تأثير شروط حدية وشروط دخول عامة)

Rawan Y. Mokhtar, Mohamed M. Tawfik and Mohamed Nabil Sabry

KEYWORDS:
Forced convection
Laminar flow
Arbitrary boundary conditions
Arbitrary inlet profile
Rectangular ducts
Compact thermal model
Flexible profile.

الملخص العربي:- تم دراسة نمذجة انتقال الحرارة بالحمل القسري تحت تأثير شروط حدية وشروط دخول عامة من أجل تجاوز الحالات التقليدية ولكن غير الواقعية من الشروط المنتظمة (تدفق حراري منتظم أو درجة حرارة منتظمة) ودرجة حرارة منتظمة عند المدخل. تم تعميم النموذج المقترح والمعروف بالنموذج الحراري المدمج المبني على الأشكال المرنة والمستخدم من قبل في دراسة الأنابيب ذات المقطع الدائري لكي يتعامل مع الأنابيب ذات المقطع المستطيل. تم تطبيق النموذج المقترح على سريان رقائقي تام التطور هيدروديناميكيا ولكن ليس حرارياً. هذا النموذج يعطي مميزات واضحة عن النموذج التقليدي المعتمد على معامل انتقال الحرارة بالحمل والذي لا تتوفر له علاقات رياضية إلا للشروط المنتظمة سواء كانت عند الجدار أو المدخل. يتعامل النموذج المقترح بفاعلية مع المسائل ذات الشروط غير المنتظمة مثل مسائل انتقال الحرارة المركب. ميزة جوهرية لهذا النموذج هو أنه يستخدم معاملة شبه تحليلية ومن هنا تكون النتائج ذات دقة عالية تقارن بتلك التي يتم الحصول عليها من برامج CFD ولكن مع وقت أقل لوحدة المعالجة المركزية. تم مقارنة النتائج التي تم الحصول عليها من النموذج المقترح مع نتائج برنامج Ansys Fluent. المقارنة وضحت أن النموذج الحراري المدمج المبني على الأشكال المرنة جدير بالثقة. أقصى خطأ كان 0.01 °C لفرق درجة حرارة بين المدخل والمخرج يصل إلى 50 °C. وبناءاً على المقارنة السابقة تم استخدام طريقة الأشكال المرنة لحل مسائل ذات شروط حدية وشروط دخول مختلفة.

***Abstract*— Modeling the forced convection heat transfer with arbitrary boundary conditions and inlet temperature profile was studied in order to go beyond the classic, but unrealistic cases of imposed uniform heat flux or wall temperature as well as a flat temperature at the inlet. The proposed approach, known as the Flexible Profile Compact Thermal Model (FP-CTM), which has been proposed earlier to treat circular cross-section ducts, is generalized here to treat ducts with a rectangular cross-section. It is applied to the laminar hydrodynamically fully developed flow but thermally developing. It offers significant advantages over the traditional model of convective heat transfer coefficient (HTC), for which correlations only exist for uniform boundary conditions and inlet profile. The proposed approach makes it more efficient when dealing with problems with non-uniform conditions such as conjugate heat transfer problems. A critical advantage of this approach is that it uses a semi-analytic treatment to produce highly accurate results that are comparable to those produced by commercial CFD tools but with significantly less CPU time. Results obtained from the proposed approach, i.e. FP-CTM were compared with that obtained from Ansys Fluent. The comparison has shown that FP-CTM is very reliable. The maximum error compared with Fluent solver results was 0.01 °C for a temperature range between the inlet and outlet of about 50 °C. Based on the preceding comparison, the FP approach was used to solve different problems with different**

Received: (21 April, 2020) - Accepted: (23 August, 2020)

R. Y. Mokhtar is with Mansoura University, Mechanical Power Engineering Dpt., Mansoura, Egypt (e-mail rawanyasser23@gmail.com).

M. M. Tawfik is with Mansoura University, Mechanical Power Engineering Dpt., Mansoura, Egypt (e-mail m_tawfik@gmail.com).

M. N. Sabry, Pr., is with Mansoura University, Mechanical Power Engineering Dpt., Mansoura, Egypt (e-mail mnabil.sabry@gmail.com).

boundary conditions (uniform and linear heating) and inlet profiles (flat and non-flat inlet) using significantly fewer computing resources.

I. INTRODUCTION

FORCED convection appears in many practical applications such as heat exchangers design, design of cooling systems in integrated circuits, design of fins, and design of the cooling system for turbine blades. Although forced convection is not a new topic (actually the first attempt to solve laminar forced convection in circular ducts was by Graetz in 1883 [1]), there are still unsolved problems related to this domain such as cases with non-uniform boundary conditions (BCs) for example in conjugate problems. Available correlations for the heat transfer coefficient (HTC) are all based on either uniform wall heat flux or uniform wall temperature. Using HTC outside its domain of validity may cause noticeable errors. In some applications, such as turbines cooling [2], it is essential to get accurate results for turbine safety and reliability. An alternative is the 3D CFD simulation. Although this method gives very accurate and reliable results, it is not suitable for large systems composed of many components because of the high computational time required.

In this study, a new method is proposed, which is a bridge between the oversimplified HTC model and complicated CFD simulation. This method, which is known as the Flexible Profile Compact Thermal Model (FP CTM), allows using non-uniform conditions as well as uniform ones. It also has the advantage of allowing arbitrary inlet conditions. Another advantage of the new approach is its flexibility in selecting the required accuracy, which can go from the low HTC accuracy to the accuracy of CFD simulation. The new approach can also deal with conjugate problems with significantly less computational time than 3D CFD simulation. Almost all publications in the literature for convection problems consider uniform conditions; for example, Aparecido and Cotta [3] developed an analytic solution for forced convection in a rectangular duct with a uniform wall temperature and fully developed velocity profile. Morini [4] developed an analytic solution for laminar forced convection in a rectangular duct with axially uniform heat flux and circumferentially uniform temperature BCs. The solution is valid in the fully developed thermal zone. Hooman and Merrikh [5] studied forced convection in a rectangular duct with uniform heat flux BCs and thermally and hydrodynamically fully developed flow. Also, Smith and Nochetto [6] performed numerical analysis for laminar convection in rectangular ducts for aspect ratio from 1 to 100 and also for parallel plates. They used in their analysis axially uniform heat flux with circumferentially uniform temperature BCs. Also, Avci and Aydin [7] used finite volume method to study thermally developing forced convection in a microtube. Hooman et al. [8] included viscous dissipation in their study of forced convection in a rectangular duct with isothermal BCs. Bennett [9] investigated forced convection in rectangular ducts using three uniform BCs, constant temperature, constant heat flux, and constant axial heat flux with constant peripheral temperature. Zukowski [10] studied laminar forced convection in a square duct with different combinations of constant temperature heated and adiabatic walls. In all these studies, Nusselt number, which is the dimensionless representation of HTC, is calculated to model this set of problems.

Although the use of HTC in thermal analysis is widespread, it has many defects. First, the derived formula of HTC is only valid for the cases with the same BCs used in the derivation, which means that HTC models are BCs dependent models, which violates the Boundary Conditions Independence (BCI) criterion [11] any physically sound model should satisfy. Secondly, the most common BCs are either uniform temperature or uniform heat fluxes, none of them are realistic boundary conditions especially when dealing with conjugate problems, and it is impractical to have a formula for each BCs. Thirdly, inlet conditions used to derive HTC formulas are either flat or fully developed, of course flat inlet causes discontinuity at inlet, which is unrealistic. Fourthly, some formula used to calculate HTC may cause noticeable errors not only because of assuming uniform inlet and boundary conditions but also because of the method used to derive the formula. For example, the error in calculating the average heat transfer coefficient in the case of a uniform heat flux condition was discussed in [12]. Hence increasing attention is devoted to the use of different methods that can deal with non-uniform inlet and BCs and produce models that are independent of the imposed inlet and BCs. For example, some researchers used experimental data to get what is known as Discrete Green Function (DGF) [2], [13]. This method can predict heat transfer in problems with non-uniform BCs. The DGF is constructed using measured temperatures at different locations due to various heat flux sources located in different locations. However, obtaining DGF experimentally is not very practical, and also, the uncertainty in the measurements may cause errors in heat transfer calculations. DGF method was used in [14] to predict heat flux across the turbine tip gap.

Another approach has been proposed by Sabry in [15], [16], to overcome the above difficulties, called Flexible Profile Compact Thermal Model (FP-CTM). This approach does not suppose uniform wall heat flux q_w or uniform wall temperature T_w. It does not suppose uniform (or flat) inlet temperature profile T_{in}. All these fields (q_w, T_w and T_{in}) are supposed as space functions each one is developed over a suitable complete series. The model is a relation between the coefficients of each series, which is a matrix that would replace the single number in the HTC approach. It requires no experiments to conduct. This method was successfully applied to forced convection in circular ducts with arbitrary inlet and boundary conditions [15]. A new definition for entrance length was derived because the conventional definition of entrance length (the length beyond which the HTC doesn't change) will not be valid when the BCs are non-uniform. The new definition states that entrance length is the length beyond which the effect of inlet condition disappears. In other words, beyond entrance length the fully developed profile will take the same shape regardless of inlet profile shape. FP CTM was

also used to model conjugate problem in circular ducts [16].

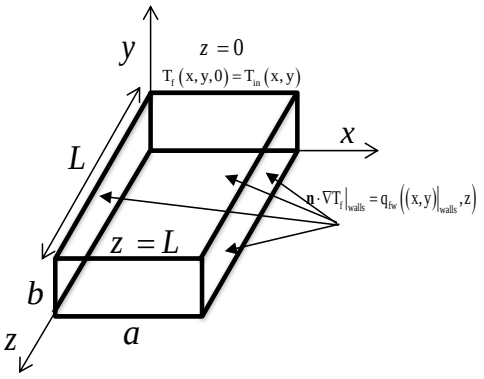

Fig. 1. Geometry of the Problem.

Two CTMs are constructed, one for fluid domain, which is laminar flow in circular pipe, and the other for solid domain. Coupling conditions at interface, which are continuity of temperature and heat flux, are applied. It is found that even if uniform heat flux is applied at outer wall neither heat flux nor the temperature distribution is uniform at the solid-liquid interface. Results obtained from CTM are in good agreement with numerical simulation using ANSYS package. In some cases, such as microchannels, ducts cross section is usually rectangular, not circular [17]–[20]. The aim of the present work is to extend the FP-CTM previously developed for circular duct to the case of laminar flow in rectangular ducts, to inherit its advantages: high precision, low CPU time and ability to treat arbitrary boundary conditions and inlet.

II. PROBLEM DESCRIPTION

Steady laminar forced convection in a rectangular duct is studied with constant physical properties. The fluid is considered to be hydrodynamically fully developed but thermally developing. Boundaries include duct walls, duct inlet $(z'=0)$, and duct outlet $(z'=L)$. The duct has dimensionless width a (in x-direction) and height b (in y-direction) as well as length L, in the z-direction, as shown in Fig. 1. All the variables are in dimensionless form.

A. Hydrodynamic problem

Laminar hydrodynamically fully developed flow under the action of a pressure gradient $\frac{dP'}{dz'}$, subject to the classical no-slip boundary condition, is considered. The velocity profile is thus composed of a single component along the duct axis $w'(x', y')$. Axial velocity obeys the Navier–Stokes equation in the z-direction, in which convective term identically vanishes due to the fully developed assumption:

$$\frac{\partial^2 w'}{\partial x'^2}+\frac{\partial^2 w'}{\partial y'^2}=\frac{1}{\mu}\frac{dP'}{dz'}=-C \tag{1}$$

where μ is the dynamic viscosity and C is a constant. This is to be solved within the plane (x', y') together with the non-slip boundary condition at the walls of the duct:

$$w'|_{walls}=0 \tag{2}$$

The pressure gradient will be expressed in terms of velocity head and friction coefficient F, using the classical model:

$$\left|\frac{dP'}{dz'}\right|=\frac{F\rho U^2}{2D_h} \tag{3}$$

where D_h is the hydraulic diameter, and U is the average velocity over the cross-section. The friction coefficient can be expressed in terms of Poiseuille number Po = F Re (Re is Reynolds number). In order to transform the problem into the dimensionless form, average velocity, U, can be taken as the characteristic velocity. Any suitable characteristic length L_{ch} can be used (in this analysis, the hydraulic diameter, D_h, is taken as the characteristic length). In the sequel, all dimensionless quantities will take the same symbol as their dimensional counterpart but without the dashes. Hence, the dimensionless version of the Navier-Stokes equation (1) will take the form:

$$\frac{\partial^2 w}{\partial x^2}+\frac{\partial^2 w}{\partial y^2}=-\left(\frac{Po}{2}\right) \tag{4}$$

This is a simple Poisson's equation in 2D. It can be easily solved, together with the dimensionless BCs, numerically by a finite volume code to get the velocity field.

B. Thermal problem

Unlike the velocity profile, the temperature profile is considered to be developing, including an entrance zone followed by a thermally developed zone. The solution will address arbitrary inlet and BCs. Steady-state heat transfer in the fluid is governed by the dimensional energy equation:

$$\rho_f c_f w'\frac{\partial T_f'}{\partial z'}=k_f\left(\frac{\partial^2 T_f'}{\partial x'^2}+\frac{\partial^2 T_f'}{\partial y'^2}+\frac{\partial^2 T_f'}{\partial z'^2}\right) \tag{5}$$

where T_f' is the fluid temperature, while physical properties ρ_f (density), c_f (heat capacity) and k_f (thermal conductivity) of the fluid are all assumed constant.

In order to obtain T_f' from (5), BCs should be imposed on all boundaries, i.e., walls, as well as at fluid inlet $(z'=0)$ and outlet $(z'=L)$. However, the condition at the outlet is usually ignored in literature as it would only affect a small portion near the duct outlet, especially at high Peclet number (Pe). Boundary conditions can take any shape. Without loss of generality, it will be assumed that all imposed fields will be expressed in terms of entering heat flux at the walls:

$$k_f\left(\mathbf{n}.\nabla T_f'\right)\big|_{walls}=q_{fw}' \tag{6}$$

Notice that both wall heat flux q_{fw}' and wall temperature $T_f'|_{walls}$ are assumed totally arbitrary, none of them is considered uniform. Temperature everywhere in the fluid domain $T_f'(x', y', z')$ will be obtained, including at the walls

$T'_f|_{walls}$, as a function of q'_{fw}. This final expression, relating q'_{fw} with $T'_f|_{walls}$, is the required, flexible profile (FP) form of the compact thermal model (CTM). It will also allow us to deal with any type of boundary conditions (Dirichlet, Neumann, or Robin). Using it together with any given boundary condition of the three types would directly give both fields q'_{fw} and $T'_f|_{walls}$.

For fluid at duct inlet $(z' = 0)$:

$$T'_f(x', y', 0) = T'_{in}(x', y') \tag{7}$$

Where T'_{in} is the fluid inlet temperature profile, also assumed arbitrary (or flexible). Without loss of generality and for convenience, reference temperature will be fluid bulk temperature at inlet. Hence, by definition:

$$\int_{A'} (T'_{in}\ w')\big|_{z'=0}\, dx'dy' = 0 \tag{8}$$

where A' is the cross-sectional area of the duct. In order to non-dimensionalize the thermal problem, additional required characteristic quantities are either heat flux q_{ch} or temperature difference ΔT_{ch}, any of them can be deduced from imposed BCs. Having one of them, the other will be obtained from: $k_f \Delta T_{ch} / L_{ch} = q_{ch}$. Using this relation, the dimensionless governing equation becomes (again using the same symbols as those of dimensional variables but without the dashes):

$$Pe\ w \frac{\partial T_f}{\partial z} = \frac{\partial^2 T_f}{\partial x^2} + \frac{\partial^2 T_f}{\partial y^2} + \frac{\partial^2 T_f}{\partial z^2} \tag{9}$$

where Pe is Peclet number defined as:

$$Pe = \frac{L_{ch} U}{\alpha_f} \qquad \text{(where } \alpha_f \text{ is the thermal diffusivity)}$$

Notice that the hydraulic diameter D_h is taken as characteristic length L_{ch}.

Thermal inlet and BCs become:

$$\mathbf{n} \cdot \nabla T_f|_{walls} = q_{fw}\left((x, y)|_{walls}, z\right) \tag{10}$$

$$T_f(x, y, 0) = T_{in}(x, y) \tag{11}$$

III. METHODOLOGY

The solution of the energy equation will be split into two solutions. The first solution T_{FD} gives the fully developed profile (this solution satisfies the energy equation and imposed heat flux q_{fw} BCs only), whereas the second T_{EN} gives the entrance zone profile (this solution, when added to the fully developed solution, guarantees the satisfaction of the inlet condition). Superposing the two solutions gives the total solution to the problem.

$$T_f(x, y, z) = T_{FD}(x, y, z) + T_{EN}(x, y, z) \tag{12}$$

Fields T_{FD} and T_{EN} satisfy:

$$Pe\ w \frac{\partial T_{FD}}{\partial z} = \frac{\partial^2 T_{FD}}{\partial x^2} + \frac{\partial^2 T_{FD}}{\partial y^2} + \frac{\partial^2 T_{FD}}{\partial z^2} \tag{13}$$

$$\mathbf{n} \cdot \nabla T_{FD}|_{walls} = q_{fw} \tag{14}$$

$$Pe\ w \frac{\partial T_{EN}}{\partial z} = \frac{\partial^2 T_{EN}}{\partial x^2} + \frac{\partial^2 T_{EN}}{\partial y^2} + \frac{\partial^2 T_{EN}}{\partial z^2} \tag{15}$$

$$\mathbf{n} \cdot \nabla T_{EN}|_{walls} = 0 \tag{16}$$

$$T_{EN}(x, y, 0) = T_{in}(x, y) - T_{FD}(x, y, 0) \tag{17}$$

Noticing that the field T_{EN} has no energy source (16), then from the First Law, the bulk temperature of T_{EN} may only slightly vary from its inlet value due to axial conduction. Such variations are negligible except for vanishing Pe.

From the Second Law, temperature differences will damp out due to heat transfer within the fluid. Hence, sooner or later, this field will tend to become uniform after a certain distance from the inlet. Reference temperature may be easily adjusted to let this uniform value tend to zero. After such distance, the only remaining field would be T_{FD}. This gives another more useful definition of the entrance length and the fully developed temperature profile, applicable for non-uniform boundary conditions, for which the classical concept was unusable. This shows that the initial temperature profile has an effect that appears in T_{EN} only, which gradually vanishes when fluid progresses in the duct. Hence a more rational definition of the entrance length would be the distance required for the field component T_{EN} to reach, for example, 1% of its value at the inlet. The remaining field T_{FD} is thus the fully developed profile, even though it may change along the duct because heating is not uniform.

IV. SEMI-ANALYTIC SOLUTION OF THE THERMAL PROBLEM

Semi-analytic solution means that we will apply an analytical pretreatment to the problem leading to a reduced one that can be easily solved numerically, i.e., requiring much fewer computing resources than if the problem was considered fully numerical.

The heat source at the wall q_{fw} is an arbitrary function of space, in terms of which the general solution needs to be obtained. Heat is assumed to be added symmetrically at the upper and lower walls only. Other vertical walls are assumed adiabatic. The case where all walls are heated could be obtained from this one by superposition, which allows a certain degree of freedom if heating was different on vertical and horizontal walls. In order to obtain the general solution, it would be normal to develop q_{fw} over a complete functional series in z. Each term in the series represents a specific excitation for which we can find a solution, i.e., corresponding temperature field. Superposing all solutions would constitute the general solution to any arbitrary heat source. The expansion could be in terms of Taylor or Fourier series or any other convenient series capable of representing the heat source q_{fw} with rather few terms. Taking Taylor series, truncated after N terms:

$$q_{fw}(z) = (\mathbf{n} g \nabla T)\big|_{y=0,b} = \sum_{i=0}^{N} q_{f,i}\, z^i; \quad (\mathbf{n} g \nabla T)\big|_{x=0,a} = 0 \tag{18}$$

As for inlet, the inlet profile can take any shape. There is no restriction on it, contrary to classical approaches where it is systematically assumed flat. So, the remaining condition in equation (11). Condition at the outlet (z=L) is ignored, as is usually the case in the literature.

A. Fully developed solution

The fully developed part of the temperature field will be obtained in terms of coefficients $q_{f,i}$, using the following general form:

$$T_{FD}(x,y,z)=\sum_{i=0}^{N+1} f_i(x,y)\, z^i \tag{19}$$

Substituting all series developments (18), and (19) in the partial differential equation (13) and the boundary condition (14), equating like powers of z to zero gives us:

$$\frac{\partial^2 f_i}{\partial x^2}+\frac{\partial^2 f_i}{\partial y^2}=S_i(x,y) \tag{20}$$

$$S_i(x,y)=(i+1)\,Pe\, w(x,y)\, f_{i+1}(x,y)-(i+2)(i+1) f_{i+2}(x,y) \tag{21}$$

$$\mathbf{n}\cdot\nabla f_i\big|_{y=0,b}=q_{f,i};\quad \mathbf{n}\cdot\nabla f_i\big|_{x=0,a}=0 \tag{22}$$

This system of equations will be solved recursively from the highest value of i downwards (from i=N+1 to i=0). For each value of i, it is only needed to solve the 2D Poisson's equation for the same geometry and same type of boundary conditions; only source functions are different. But before that, some essential notes must be mentioned.

Note 1: Consistency condition

Integrating both sides of (20) over the cross-sectional plane of the duct, using Gauss theorem and boundary condition (22) we get:

$$2aq_{f,i}=\int_A S_i(x,y)\,dx\,dy \tag{23}$$

where A is the cross-sectional area.

Using (23), and defining $S_{i,avg}$ as the area average of S_i, noting that the above equation is in a dimensionless form, we conclude that:

$$S_{i,avg}=\left(\frac{2}{b}\right) q_{f,i} \tag{24}$$

Hence, $S_i(x, y)$ is not arbitrary since it should satisfy (24).

Note 2: Arbitrary constants

The unknown function $f_i(x, y)$ appearing in differential equation (20) and boundary condition (22) always appears differentiated. Hence, its solution is only defined up to an arbitrary additive constant. Let us temporarily designate a particular solution by $g_i(x,y)$, then:

$$f_i(x,y)=g_i(x,y)+C_i \tag{25}$$

where C_i is a yet arbitrary constant. The value of this constant will be fixed while solving the equation of the lower order value of i. In fact, $S_{i-1}(x, y)$ contains $f_i(x, y)$, which in turn contains C_i. By imposing the condition (24) for i-1, we immediately get the value of C_i.

Note 3: The reference temperature

All values of integration constants C_i from i=N+1 to i=1 can be obtained using the procedure depicted in the previous note as a function of $q_{f,i}$. As for C_0, its value should be fixed otherwise. Notice that, by virtue of (19) the function $f_0(x, y)$ is simply the inlet profile of the fully developed temperature field $T_{FD}(x, y, 0)$. Hence, the constant C_0 will be split into the sum of two constants. One of them will counterbalance the bulk temperature of g_i', the other will simply be the bulk temperature of the fully developed part at inlet T_{FDb}. The later will be fixed after solving for the entrance length part.

$$C_0=-\frac{\int_A g_0'(x,y)w(x,y)dxdy}{\int_A w(x,y)dxdy}+T_{FDb} \tag{26}$$

From the previous discussion, it can be concluded that we have N+2 coefficients C_i to obtain from i=0 to N+1 and also N+2 conditions, which are to satisfy reference temperature condition (26) in addition to the N+1 conditions (24) applied for i=0 to N. This explains why expansion (19) has been truncated after i = N+1. In this study, numerical method (finite volume method) is used to solve the set of 2D Poisson's equations.

Defining a suitable metric for the wall temperature $T_{f,FD}$ (either the average or the maximum or any other metric), we get an expression for it from (19) in the form of a polynomial in z. Coefficients of this polynomial can be represented as a vector $\mathbf{T}_{f,FD}$. Above sketched solution relates these coefficients to the vector containing coefficients of the polynomial representing wall heat flux $\mathbf{q}_f$ in the form of the matrix relation:

$$\mathbf{T}_{f,FD}=\mathbf{R}_{f,FD}\,\mathbf{q}_f \tag{27}$$

where $\mathbf{R}_{f,FD}$ is the thermal resistance matrix that generalizes the scalar HTC (or precisely its inverse).

The solution of the fully developed forced convection problem in a straight duct of the rectangular cross-section due to arbitrary wall heat flux is thus obtained. The original 3D convection/diffusion problem has been transformed into a set of simple 2D Poisson's equations with given boundary conditions. The obtained field still does not satisfy inlet conditions. Hence it is only valid sufficiently far from the inlet. Thus, entrance solution is obtained in the next section in order to satisfy inlet conditions.

B. Entrance solution

The entrance field T_{EN} will be expanded over a series that decays exponentially along the duct length; thus, the only field that remains at a long distance from entry is the fully developed field.

$$T_{EN}(x,y,z)=\sum_i A_i\, h_i(x,y)\, e^{\frac{-\lambda_i z}{Pe}} \tag{28}$$

where constants A_i and λ_i and functions h_i are yet to be determined. It should be noted that although the entrance field has no heating source at the wall (16), its bulk temperature may still vary along z due to axial conduction at both tube ends. The above equation (28) means that the bulk temperature of the entrance field is assumed zero at infinity, i.e. sufficiently far from the inlet. The bulk temperature of the entrance field at inlet T_{ENb} is not necessarily zero. To get an expression for it, let us split each expansion function into one that has zero bulk $\bar{h}_i(x,y)$ and a constant bulk temperature h_{ib}:

$$h_i(x,y) = \bar{h}_i(x,y) + h_{ib};\ h_{ib} = \frac{\int_A w(x,y) h_i(x,y)\,dxdy}{\int_A w(x,y)\,dxdy} \quad (29)$$

Hence, from (28) and (29) we can easily deduce that:

$$T_{ENb} = \sum_i A_i h_{ib} \quad (30)$$

Substituting (28) into the partial differential equation (15) and equating coefficients of same exponential power gives the set of differential equations:

$$\frac{\partial^2 h_i}{\partial x^2} + \frac{\partial^2 h_i}{\partial y^2} + \lambda_i \left(w + \frac{\lambda_i}{Pe^2} \right) h_i = 0 \quad (31)$$

Which should be solved together with the boundary condition (corresponding to (16)):

$$\mathbf{n} \cdot \nabla h_i \big|_{walls} = 0 \quad (32)$$

There is a trivial solution to the system (31) and (32), which is simply $h_i(x, y) \equiv 0$. We are seeking other non-trivial solutions, which is typically an eigenvalue problem λ_i being eigen values, and h_i are eigenfunctions. It is to be noted that for high Pe, the second term between parentheses in the LHS of equation (31) can be neglected, which transforms it into a Sturm-Liouville problem having an orthogonal set of eigenfunctions. Physically, this means neglecting axial conduction through the fluid domain if fluid velocity is high enough, which is the case for most practical problems. In the general case, considered here, where Pe is not necessarily large, eigenfunctions still exist but are no longer orthogonal.

To obtain eigenvalues and eigenfunctions of (31), it is possible to transform it into an algebraic eigenvalue problem through discretization. The resulting eigenvalue problem can be solved using any standard numerical computational modeling software (such as Matlab, Scilab or Octave). Finally, in order to obtain constants A_i, the inlet boundary condition is to be satisfied.

Let us rewrite (17) as:

$$T_{in} - \left[T_{FD}(x,y,0) - T_{FDb} \right] = \left(T_{FDb} + T_{ENb} \right) + \sum_i A_i \bar{h}_i(x,y) \quad (33)$$

The term between squared brackets of (33) is the part having no bulk of T_{FD} (x, y, 0), i.e. of the function $f_0(x, y)$ obtained above for fully developed flow. It depends linearly on all expansion coefficients $q_{f,i}$ for i=0 to N, which are all known, since the second term on the RHS of (33) also has zero bulk temperature, we deduce:

$$T_{FDb} + T_{ENb} = 0 \quad (34)$$

Hence, obtaining coefficients A_j is straightforward by multiplying both sides of (33) by $w(x,y)\bar{h}_i(x,y)$ and integrating over the cross-sectional area A. Using obtained A_i, T_{ENb} can be directly obtained from (30) and hence T_{FDb} from (34).

Temperature field T_{EN} can thus be obtained; hence the temperature at any point in the duct is obtained from (12).

Defining a suitable metric for the wall temperature (either the average or the maximum or any other metric) $T_{f,EN}$, we get:

$$T_{f,EN}(z) = \sum_{i=1}^{M} T_{f,EN,i}\, e^{\frac{-\lambda_i z}{Pe}} \quad (35)$$

where M is the maximum number of eigenvalues considered. It is expected to have very few terms as the exponential decays rapidly with λ_i.

From (27) and (35) the average wall temperature on the

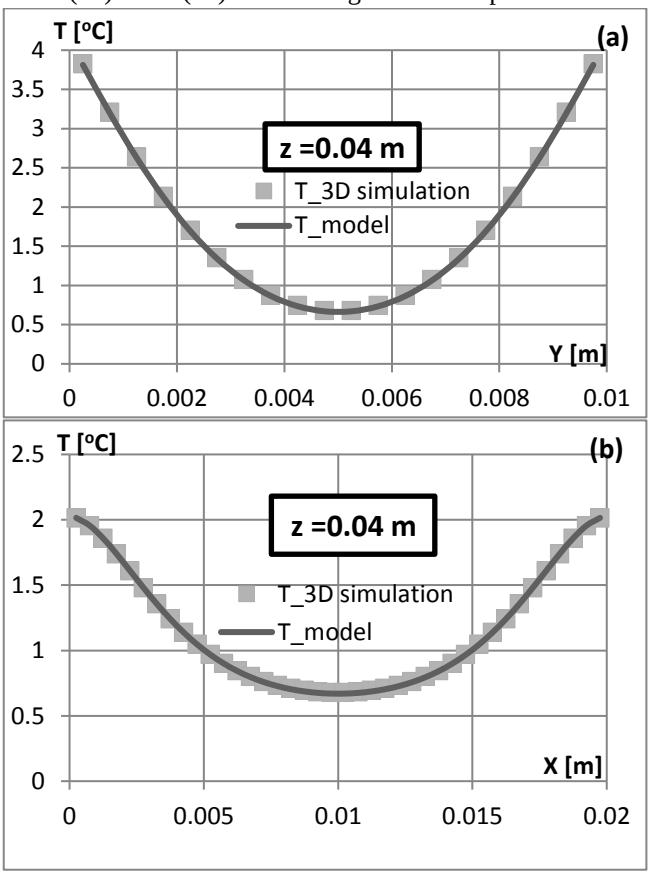

Fig. 2. Comparison between the proposed model and 3D simulator in the entrance zone as a function of y (a) and x (b).

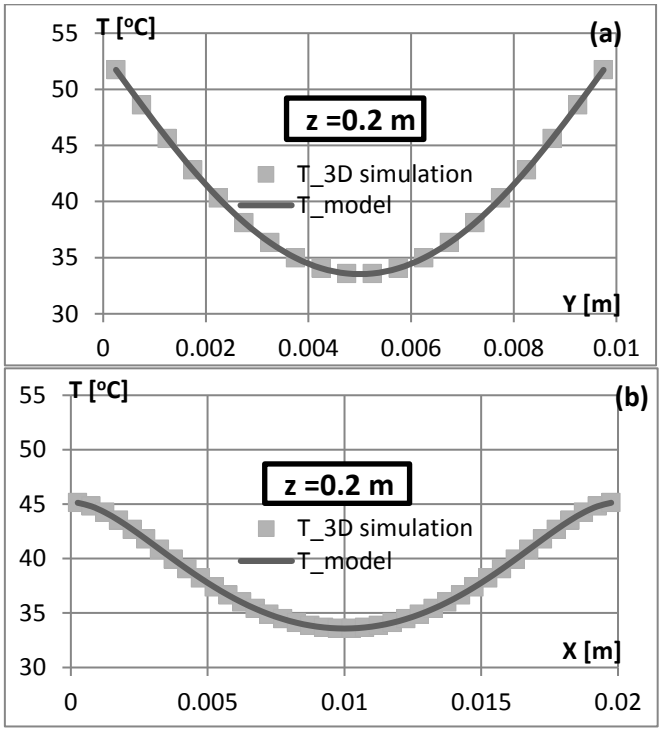

Fig. 3. Comparison between the proposed model and 3D simulator in the fully developed zone as a function of y (a) and x (b).

horizontal walls and the vertical walls will be obtained, based on which CTM will be constructed as it will be shown in VI.

V. VALIDATION

In order to test the proposed model, i.e. FP model, a case study is performed and compared with 3D simulator (Ansys Fluent) results. Air is used as the working fluid with constant physical properties. The aspect ratio of the rectangular cross-section duct equals 2. The dimension of the rectangular duct

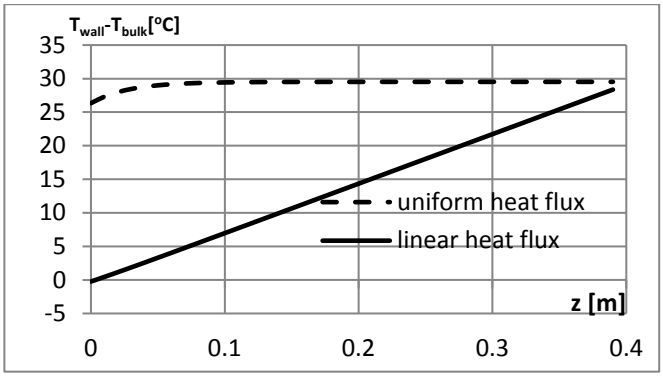

Fig. 4. T_{wall}-T_{bulk} for two different heating distributions, uniform and linearly heating.

was 0.01, 0.02, 0.4 m. For simplicity, heating was on the top and bottom walls only. Heating on the other two walls can be done with the same approach. Heating on only two walls allows a degree of freedom to treat cases with different heating rates on horizontal and vertical walls. The air was flowing at a Peclet number Pe=40. The characteristic length L_{ch} is hydraulic diameter, (D_h =4A/p) and the characteristic heat flux, q_{ch} equals 10 W/m^2.

Linear heating was used in the analysis (q_{1H}*z where q_{1H} = 1). Again, for simplicity, flat profile was used at the inlet (0 °C). The cells of the mesh were square with dimensions 1x1 mm^2. This mesh was suitable for the used CPU. The maximum error compared with Fluent solver results was 0.01 °C for a temperature range between inlet and outlet of about 50 °C. Temperature profiles are shown in Fig. 2 for a duct cross-section in the entrance zone. Fig. 3 shows temperature profiles in the fully developed zone. Profiles are given as a function of either x or y, both for a line passing through the duct center.

VI. RESULTS AND DISCUSSION

Fig. 4 compares $T_{wall} - T_{bulk}$ for a flat inlet temperature field (0 °C) and two different heating distributions: uniform (q_{0H} =30) and linearly increasing (q_{1H} =1). As expected, the difference between the wall temperature and the bulk temperature is constant in the fully developed zone in the case of uniform heating. As can also be expected for linear heating, the difference between the wall temperature and the bulk temperature is increasing linearly.

Two different inlet profiles are shown in Fig. 5, a flat (0 °C) and a non-flat profiles ($-2*1000*T_{ch}*h_2(x,y)$ °C) (dotted lines). They were applied for the same linearly increasing heating profile. In the same figure is shown the fully developed profile at the inlet (solid line) for reference. The

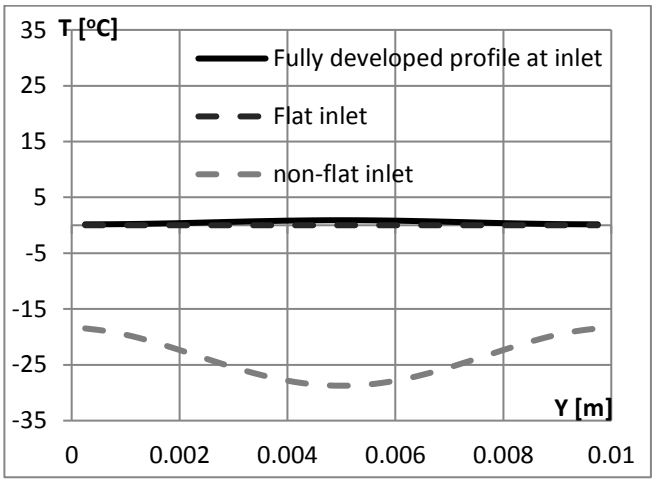

Fig. 5. Temperature profiles at inlet.

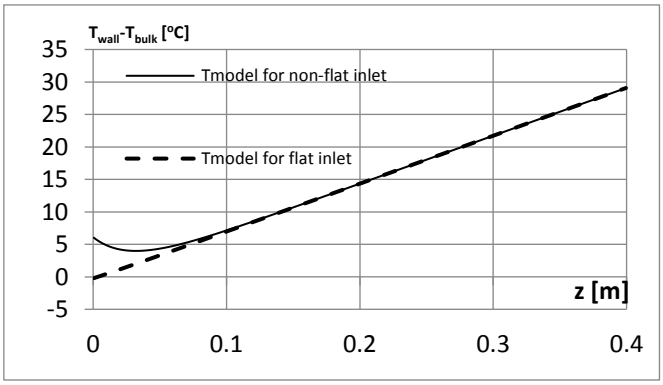

Fig. 6. Temperature difference for two different inlet profiles with linear heating.

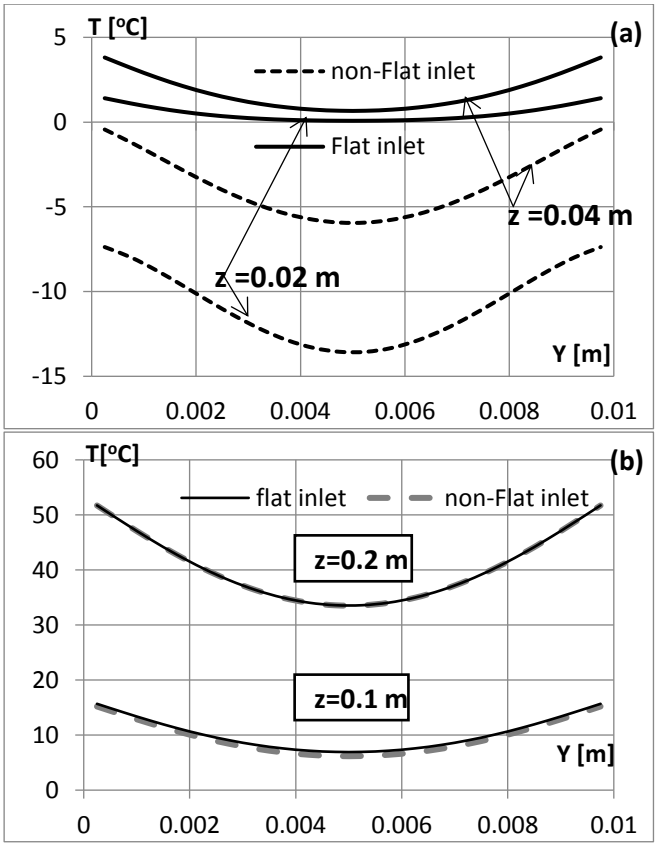

Fig. 7. Temperature profiles at different axial positions.

values of $T_{wall}-T_{bulk}$ corresponding to both inlet profiles are shown in Fig. 6. They are different only in the entrance region. The difference gradually vanishes as fluid progresses in the duct. This confirms what was stated early in [15] about entrance length. The inlet profile has an effect that appears for some distance from the inlet. Beyond that distance temperature profile is the same for a given heating profile.

For flat inlet, there is almost no entrance length. This means flat inlet, in this case, is almost the fully developed profile at the inlet. This is confirmed by Fig. 5.

As for non-flat inlet, the values of $T_{wall}-T_{bulk}$ first decrease then start increasing again. This is because heating near the inlet is minimal (almost vanishing), while radial conduction inside fluid layers dominates in this region. Identical results were obtained by Fluent solver. This plays a significant role in decreasing the difference between wall and bulk temperatures. As the fluid progresses, heating from walls increases and starts to affect the fluid temperature profile.

Fig. 7 depicts temperature profiles across duct section at different sections along the duct, both in the entrance region (a) and the fully developed region (b), confirming what was stated above about the entrance length, regarding Fig. 6.

The results were obtained for a relatively short duct ($L/D_h = 30$), the CPU time required for Ansys Fluent simulation is around six minutes to solve the whole problem (64 seconds for the thermal problem) while it is nearly two seconds for the proposed approach. Increasing the duct length will considerably increase the CPU time for any CFD simulator while it will remain the same for the proposed approach.

Another important advantage of the proposed approach is that once the model is constructed; any other set of boundary conditions can be applied with much less time, as reported at the end of this section, compared to CFD simulator which will solve the equations for each time the boundary conditions change.

The FP approach combines between the accurate results and the reasonable computing time required to get the solution. These advantages stem from the semi-analytical solution of the energy equation using the flexible profiles; the resulting equations (2D Poisson's equations for the fully developed field and an eigenvalue problem for the entrance field) are much simpler compared to the full 3D energy equation. So, this makes this approach very useful when dealing with large scale problems that require highly accurate results.

FP CTM construction

Using (27) and (35) the average wall temperature on the horizontal and the vertical walls can be obtained, based on which FP CTM is constructed. But before that the exponential function is approximated with a polynomial of the fourth order in z to able to add the two vectors of coefficients.

$$\begin{bmatrix}\mathbf{T_{wallH}}\\ \mathbf{T_{wallV}}\end{bmatrix}=\begin{bmatrix}\mathbf{R}_{HH} & \mathbf{R}_{HV}\\ \mathbf{R}_{VH} & \mathbf{R}_{VV}\end{bmatrix}\begin{bmatrix}\mathbf{q_{wallH}}\\ \mathbf{q_{wallV}}\end{bmatrix}+\begin{bmatrix}\mathbf{E}_H\\ \mathbf{E}_V\end{bmatrix}\begin{bmatrix}A_1\\ A_2\\ A_3\end{bmatrix}$$

where $\mathbf{T_{wallH}}$ and $\mathbf{T_{wallV}}$ are two vectors representing the coefficients of $\left[z^0, z^1, z^2, z^3, z^4\right]$. This means the average wall temperature on the horizontal and the vertical walls are two polynomials in axial position (z). The coefficients of each polynomial are presented in vector form ($\mathbf{T_{wallH}}$ and $\mathbf{T_{wallV}}$).

$\mathbf{R}_{HH}$, $\mathbf{R}_{HV}$, $\mathbf{R}_{VH}$, $\mathbf{R}_{VV}$ are four matrices representing the fully developed field. $\mathbf{R}_{HH}$ and $\mathbf{R}_{HV}$ represent the coefficients of the horizontal wall temperature in case of imposing heat flux (all of its coefficients equal one) on the horizontal and vertical walls respectively while $\mathbf{R}_{VH}$ and $\mathbf{R}_{VV}$ represent the coefficients of the vertical wall temperature in case of imposing heat flux (all of its coefficients equal one) on the horizontal and vertical walls respectively:

$$\mathbf{R}_{HH}=\begin{bmatrix}0.178586 & -0.00191Pe+\frac{0.047512}{Pe}\\ \frac{2.649634}{Pe} & 0.178586+\frac{2.63271}{Pe^2}\\ 0 & \frac{1.324817}{Pe}\\ 0 & 0\\ 0 & 0\end{bmatrix};\mathbf{R}_{HV}=\begin{bmatrix}0.063226 & -0.00196Pe+\frac{0.023756}{Pe}\\ \frac{1.324817}{Pe} & 0.063226+\frac{1.316355}{Pe^2}\\ 0 & \frac{0.662408}{Pe}\\ 0 & 0\\ 0 & 0\end{bmatrix}$$

$$\mathbf{R}_{VH}=\begin{bmatrix}0.126451 & -0.00393Pe+\frac{0.101902}{Pe}\\ \frac{2.649634}{Pe} & 0.126451+\frac{2.63271}{Pe^2}\\ 0 & \frac{1.324817}{Pe}\\ 0 & 0\\ 0 & 0\end{bmatrix};\mathbf{R}_{VV}=\begin{bmatrix}0.322158 & -0.00891Pe+\frac{0.050951}{Pe}\\ \frac{1.324817}{Pe} & 0.322158+\frac{1.316355}{Pe^2}\\ 0 & \frac{0.662408}{Pe}\\ 0 & 0\\ 0 & 0\end{bmatrix}$$

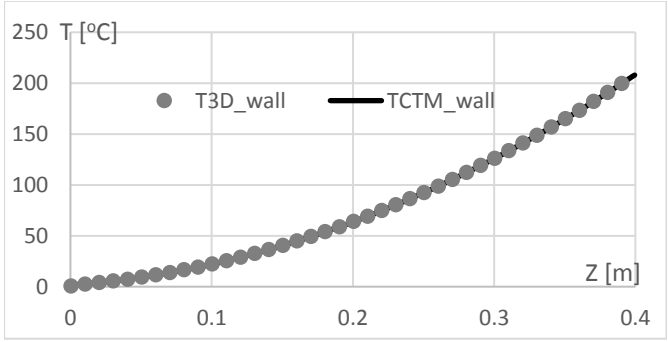

Fig. 8. The average wall temperature on the horizontal walls.

$\mathbf{q_{wallH}}$ and $\mathbf{q_{wallV}}$ are two vectors representing the coefficients of the horizontal and vertical wall heat fluxes polynomials.

$$\mathbf{q_{wallH}}=\begin{bmatrix}q_{0H}\\ q_{1H}\end{bmatrix};\mathbf{q_{wallH}}=\begin{bmatrix}q_{0V}\\ q_{1V}\end{bmatrix}$$

$\mathbf{E}_H$ and $\mathbf{E}_V$ are two matrices representing the entrance field:

$$\mathbf{E}_H=\begin{bmatrix}1.4164e\text{-}09 & -0.0004526 & -0.0015552\\ \frac{-7.1665e\text{-}09}{Pe} & \frac{0.004736}{Pe} & \frac{0.01705}{Pe}\\ \frac{1.5519e\text{-}08}{Pe^2} & \frac{-0.016744}{Pe^2} & \frac{-0.061385}{Pe^2}\\ \frac{-1.6142e\text{-}08}{Pe^3} & \frac{0.02393}{Pe^3} & \frac{0.088718}{Pe^3}\\ \frac{6.522e\text{-}09}{Pe^4} & \frac{-0.011905}{Pe^4} & \frac{-0.044467}{Pe^4}\end{bmatrix};\mathbf{E}_V=\begin{bmatrix}0.0083941 & -0.0020441 & 9.8572e\text{-}10\\ \frac{-0.042613}{Pe} & \frac{0.021634}{Pe} & \frac{-1.0796e\text{-}08}{Pe}\\ \frac{0.092279}{Pe^2} & \frac{-0.076487}{Pe^2} & \frac{3.8868e\text{-}08}{Pe^2}\\ \frac{-0.095984}{Pe^3} & \frac{0.10931}{Pe^3} & \frac{-5.6176e\text{-}08}{Pe^3}\\ \frac{0.03878}{Pe^4} & \frac{-0.054383}{Pe^4} & \frac{2.8156e\text{-}08}{Pe^4}\end{bmatrix}$$

The constructed FP CTM can deal with different combinations of uniform and linear heating as well as different inlet profiles. With just a fraction of second (0.01 second) any case can be obtained, unlike the commercial CFD software which need to solve the problem from beginning at each time the inlet or the wall conditions change.

CTM is tested using the following conditions:
q_{0H}, q_{1H}, q_{0V}, q_{1V} values are 2, 0, 0, 2 respectively; the inlet profile is flat (0 °C).

Fig. 8 compares the average temperature for the horizontal walls obtained from the constructed model with that obtained from Ansys Fluent. The maximum absolute error is 1.2 °C for a temperature range between inlet and outlet of about 200 °C. This error results from approximating the exponential function to polynomial one and also truncating the entrance series solution after three terms due to the fast decay of the exponential function.

VII. CONCLUSION

The previously proposed approach, i.e. Flexible Profile Compact Thermal Model (FP-CTM) has been extended to deal with forced convection in rectangular ducts. It has maintained the main advantages which are:

- The ability to deal with any arbitrary wall boundary conditions (non-uniform wall heat flux or non-uniform wall temperature).
- The ability to deal with any inlet temperature profile, not necessarily flat inlet.
- The ability to obtain detailed temperature distribution inside the duct with any precision required.
- A very high computational efficiency since a very small error compared to standard Finite Volume code for a computational time that is significantly less.

These advantages stem from the analytical pretreatment of the energy equation in its 3D form, resulting in a quite simple 2D problem to be solved numerically to obtain the temperature field everywhere in the whole domain. Results were cast in the form of a matrix that can be reused for any other set of boundary conditions to predict the temperature field using a negligible CPU time.

NOMENCLATURE

Latin symbols

A'	Dimensional cross-section area of the duct	m^2
A	Dimensionless cross-section area of the duct	-
A_i	Expansion coefficient of Eq. (28)	-
a	Dimensionless rectangle width	-
b	Dimensionless rectangle depth	-
C_i	Additive constant, see Eq. (25)	-
c_f	Heat capacity	J/kg.K
D_h	Hydraulic diameter	m
F	Friction coefficient	-
$g_i(x,y)$	Particular solution of Eq. (20)	-
h_i	Expansion function of Eq. (28)	-
k	Thermal conductivity	W/m.K
L	Duct length	-
M	Number of terms of Eq. (35)	-
N	Number of terms of Eq. (18)	-
P'	Pressure	Pa
Pe	Peclet number	-
Po	Poiseuille number	-
q	Wall heat flux	W/m^2
R	Thermal resistance matrix	-
Re	Reynolds number	-
T'	Dimensional temperature	°C
T	Dimensionless temperature	-
U	Average velocity	m/s
w'	Dimensional axial velocity	m/s
w	Dimensionless axial velocity	-
x', y'	Dimensional coordinates in the cross-section plane of the duct	m
x, y	Dimensionless coordinates in the cross-section plane of the duct	-
Z, z'	Dimensional axial coordinate	m
z	Dimensionless axial coordinate	-

Greek symbols

α	Thermal diffusivity
λ	Eigenvalue
μ	Dynamic viscosity
ρ	Fluid density

Subscripts

ch	Characteristic
EN	Entrance
f	fluid
FD	Fully Developed
H	Horizontal
in	Inlet
V	Vertical
w	wall

Abbreviations

BC	Boundary Condition
CFD	Computational Fluid Dynamics
CTM	Compact Thermal Model
FP	Flexible Profile
HTC	Heat Transfer Coefficient
2D	Two-dimensional
3D	Three-dimensional

REFERENCES

[1] L. Graetz, "Ueber die wärmeleitungsfähigkeit von flüssigkeiten," *Ann. Phys.*, vol. 254, no. 1, pp. 79–94, 1882.

[2] C. Booten and J. K. Eaton, "Discrete Green's function measurements in internal flows," *J. Heat Transfer*, vol. 127, no. 7, pp. 692–698, 2005.

[3] J. B. Aparecido and R. M. Cotta, "Thermally developing laminar flow inside rectangular ducts," *Int. J. Heat Mass Transf.*, vol. 33, no. 2, pp. 341–347, Feb. 1990.

[4] G. L. Morini, "Analytical determination of the temperature distribution and Nusselt numbers in rectangular ducts with constant axial heat flux," *Int. J. Heat Mass Transf.*, vol. 43, no. 5, pp. 741–755, Mar. 2000.

[5] K. Hooman and A. A. Merrikh, "Analytical solution of forced convection in a duct of rectangular cross section saturated by a porous medium," *J. Heat Transfer*, vol. 128, no. 6, pp. 596–600, Jun. 2006.

[6] A. N. Smith and H. Nochetto, "Laminar thermally developing flow in rectangular channels and parallel plates: uniform heat flux," *Heat Mass Transf.*, vol. 50, no. 11, pp. 1627–1637, Nov. 2014.

[7] M. Avci and O. Aydin, "Analysis of extended micro-Graetz problem in a microtube," *Sadhana - Acad. Proc. Eng. Sci.*, vol. 43, no. 7, pp. 1–9, 2018.

[8] K. Hooman, A. Haji-Sheikh, and D. A. Nield, "Thermally developing Brinkman–Brinkman forced convection in rectangular ducts with isothermal walls," *Int. J. Heat Mass Transf.*, vol. 50, no. 17–18, pp. 3521–3533, Aug. 2007.

[9] T. D. Bennett, "Laminar convection in rectangular ducts of fully developed flow," *Int. J. Heat Mass Transf.*, vol. 156, p. 119846, 2020.

[10] M. Zukowski, "Forced convection heat transfer in square duct with heated and adiabatic walls at constant axial heat flux," in *AIP Conference Proceedings*, 2019, vol. 2078, no. March.

[11] C. J. M. Lasance, "Ten years of boundary-condition- independent compact thermal modeling of electronic parts: A review," *Heat Transf. Eng.*, vol. 29, no. 2, pp. 149–168, Feb. 2008.

[12] T. D. Bennett, "A historical misperception on calculating the average convection coefficient in tubes with constant wall heat flux," *J. Heat Transfer*, vol. 141, no. 6, pp. 1–35, Jun. 2019.

[13] K. A. Batchelder and J. K. Eaton, "Practical experience with the discrete Green's function approach to convective heat transfer," *J. Heat*

Transfer, vol. 123, no. 1, pp. 70–76, Feb. 2001.
[14] V. Andreoli, D. G. Cuadrado, and G. Paniagua, "Prediction of the turbine tip convective heat flux using discrete Green's functions," *J. Heat Transfer*, vol. 140, no. 7, Jul. 2018.
[15] M. N. Sabry, "Analytic modeling of laminar forced convection in a circular duct for arbitrary boundary conditions and inlet temperature profile," *Int. J. Heat Mass Transf.*, vol. 112, pp. 933–939, Sep. 2017.
[16] M. R. Elmarghany, M. H. Mansour, A. A. Sultan, and M. N. Sabry, "Modeling of conjugate heat transfer," *Mansoura Eng. J.*, vol. 41, no. 1, pp. 16–23, 2016.
[17] A. Esmaeilnejad, H. Aminfar, and M. S. Neistanak, "Numerical investigation of forced convection heat transfer through microchannels with non-Newtonian nanofluids," *Int. J. Therm. Sci.*, vol. 75, pp. 76–86, 2014.
[18] R. Nebbati and M. Kadja, "Study of Forced Convection of a Nanofluid Used as a Heat Carrier in a Microchannel Heat Sink," in *Energy Procedia*, 2015, vol. 74, pp. 633–642.
[19] Z. Y. Ghale, M. Haghshenasfard, and M. N. Esfahany, "Investigation of nanofluids heat transfer in a ribbed microchannel heat sink using single-phase and multiphase CFD models," *Int. Commun. Heat Mass Transf.*, vol. 68, pp. 122–129, 2015.
[20] D. R. S. Raghuraman, R. T. K. Raj, P. K. Nagarajan, and B. V. A. Rao, "Influence of aspect ratio on the thermal performance of rectangular shaped micro channel heat sink using CFD code," *Alexandria Eng. J.*, vol. 56, no. 1, pp. 43–54, 2017.